

## Supporting Information

### Enhancing Broadband Blue Luminescence Efficiency and Stability in Bi<sup>3+</sup>-Doped Cs<sub>2</sub>ZnCl<sub>4</sub> Nanocrystals from STEs and Advancing Energy Applications

Xing-Yao Zhao<sup>a</sup>, Xiao-Song Zhang<sup>a,b,\*</sup>, Xiao-Kai Gong<sup>b</sup>, Xiu-Rong Yuan<sup>a</sup>, Min-Xing Chen<sup>a</sup>,  
Shu-Wei Huang<sup>b</sup>, Bao-zeng Zhou<sup>c</sup>, Jian-Ping Xu<sup>a</sup>, Lan Li<sup>a,b</sup>

<sup>a</sup>*Tianjin Key Laboratory of Quantum Optics and Intelligent Photonics, School of Science, Tianjin University of Technology, Tianjin 300384, China*

<sup>b</sup>*School of Materials Science and Engineering, Tianjin University of Technology, Tianjin 300384, China*

<sup>c</sup>*Tianjin Key Laboratory of Film Electronic & Communicate Devices, School of Integrated Circuit Science and Engineering, Tianjin University of Technology, Tianjin 300384, China*

*Corresponding author: XiaoSong Zhang\*, Email address : zhangxiaosong022@126.com*

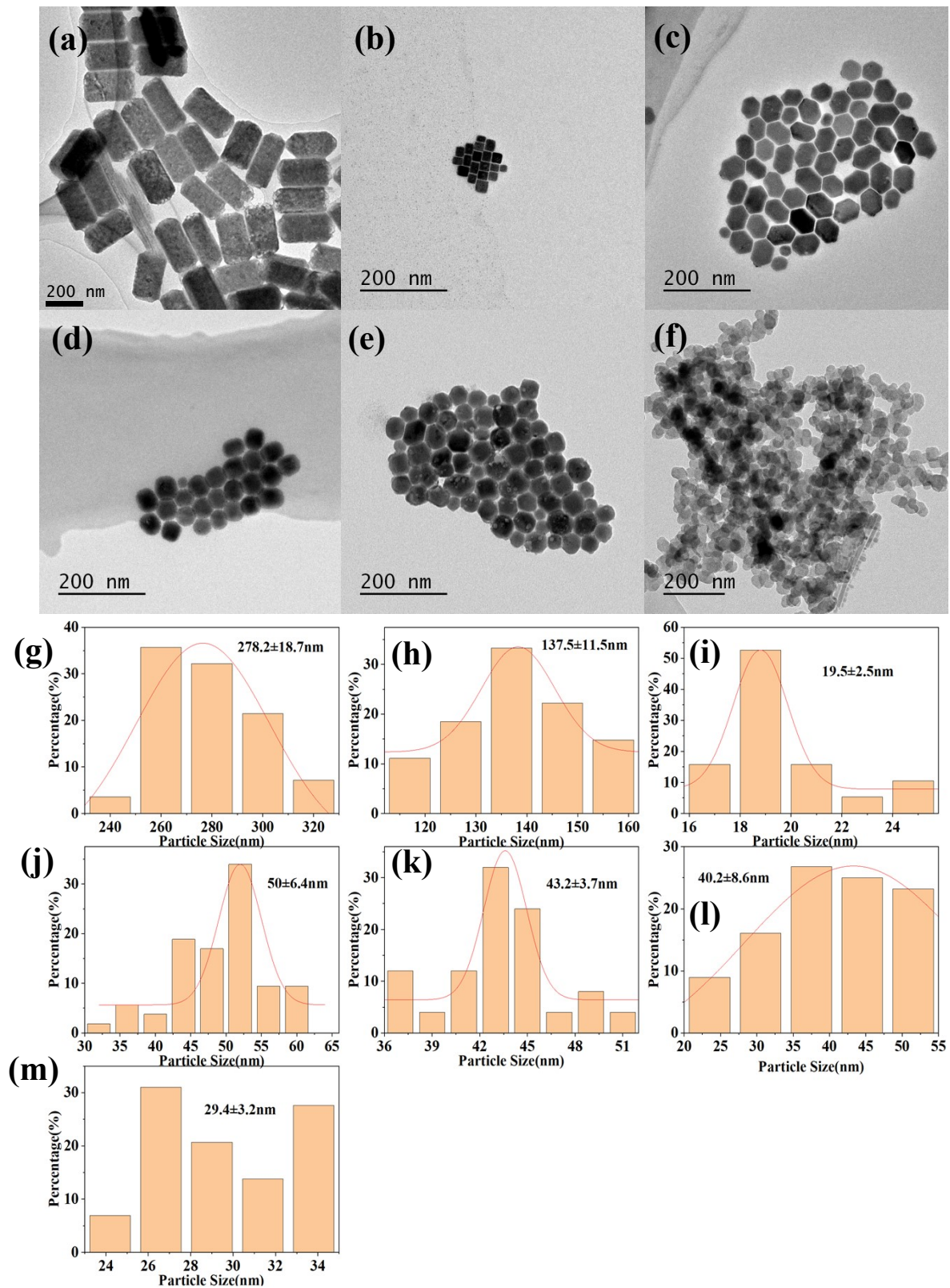


**Fig. S1.** TEM images of (a)  $\text{Cs}_2\text{ZnCl}_4$ , (b)  $\text{Cs}_2\text{ZnCl}_4:1\%\text{Bi}$ , (c)  $\text{Cs}_2\text{ZnCl}_4:3\%\text{Bi}$ , (d)  $\text{Cs}_2\text{ZnCl}_4:5\%\text{Bi}$ , (e)  $\text{Cs}_2\text{ZnCl}_4:10\%\text{Bi}$  and (f)  $\text{Cs}_2\text{ZnCl}_4:20\%\text{Bi}$  NCs. Size distribution histograms of (g)(h)  $\text{Cs}_2\text{ZnCl}_4$ , (i)  $\text{Cs}_2\text{ZnCl}_4:1\%\text{Bi}$ , (j)  $\text{Cs}_2\text{ZnCl}_4:3\%\text{Bi}$ , (k)  $\text{Cs}_2\text{ZnCl}_4:5\%\text{Bi}$ , (l)  $\text{Cs}_2\text{ZnCl}_4:10\%\text{Bi}$  and (m)  $\text{Cs}_2\text{ZnCl}_4:20\%\text{Bi}$  NCs. Figures (g) and (h) represent the length and width distribution histograms of  $\text{Cs}_2\text{ZnCl}_4$  NCs respectively.

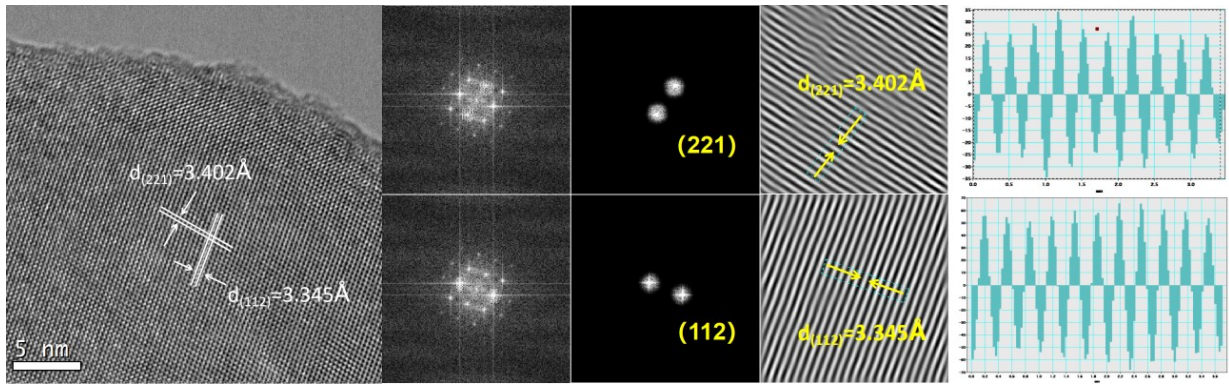


**Fig. S2.** (a) HRTEM image and (b-i) the corresponding Fast Fourier transforms (FFTs) of 3%Bi doped  $\text{Cs}_2\text{ZnCl}_4$  NCs.

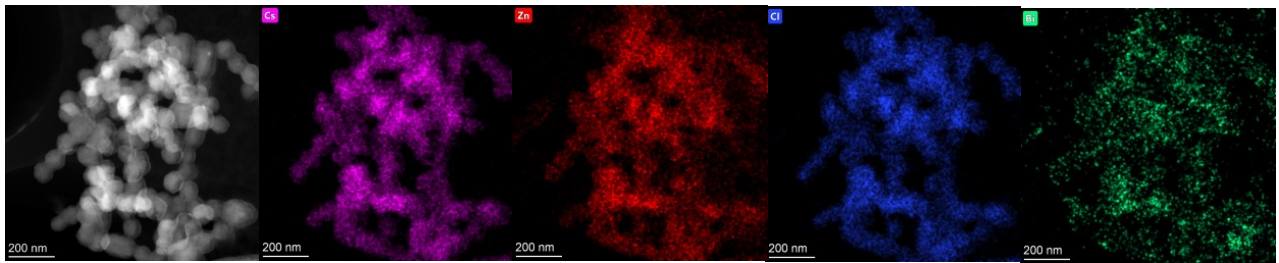


**Fig. S3.** EDS elemental mapping of Cs, Zn, Cl and Bi elements in  $\text{Cs}_2\text{ZnCl}_4:3\%\text{Bi}^{3+}$  NCs.

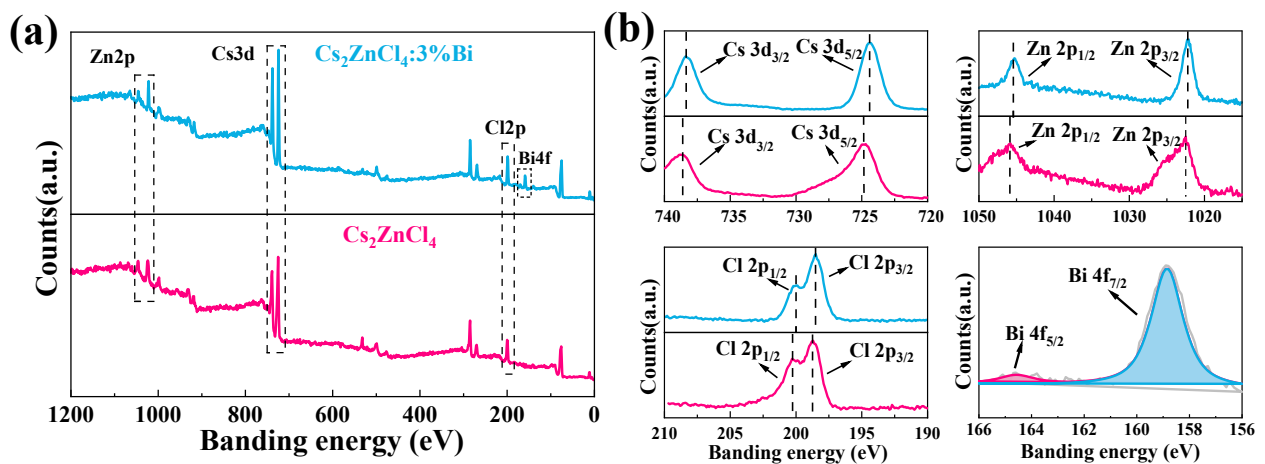


**Fig. S4.** (a) XPS spectra of  $\text{Cs}_2\text{ZnCl}_4$  NCs and  $\text{Cs}_2\text{ZnCl}_4:3\% \text{Bi}$  NCs. (b) High resolution XPS spectra of Cs 3d, Zn 2p, Cl 2p and Bi 4f.

In order to identify the elemental composition of the material and its valence state, XPS analysis was performed on undoped  $\text{Cs}_2\text{ZnCl}_4$  NCs and  $\text{Cs}_2\text{ZnCl}_4:3\% \text{Bi}$  NCs, both subjected to a charge calibration with C 1s (284.8 eV) as the reference peak. Fig. S4 shows the XPS spectra of pure  $\text{Cs}_2\text{ZnCl}_4$

NCs and Cs<sub>2</sub>ZnCl<sub>4</sub>:3% Bi NCs. The XPS spectra of the Bi-doped samples show the characteristic peaks of Cs, Zn, Cl, and Bi, while the undoped samples have no characteristic peaks of Bi<sup>3+</sup>, indicating that the Bi<sup>3+</sup>-doped samples were successfully doped with Bi<sup>3+</sup> into the lattice. In the XPS high-resolution spectra of Cs<sub>2</sub>ZnCl<sub>4</sub>:3% Bi NCs (Fig. S4b), characteristic peaks were observed at 164.6 eV and 158.8 eV, corresponding to 4f<sub>5/2</sub> and 4f<sub>7/2</sub> for Bi<sup>3+</sup>, respectively, and at 1045.2 eV and 1022.1 eV, corresponding to 2p<sub>1/2</sub> and 2p<sub>3/2</sub> for Zn<sup>2+</sup>, respectively. The analysis demonstrates that the elemental valence states of Bi and Zn in the doped NCs are stable, being +3 and +2, respectively, with no change in valence state. The electron binding energies of Cs, Zn, and Cl elements of Cs<sub>2</sub>ZnCl<sub>4</sub>:3% Bi NCs were all reduced by about 0.2 eV-0.3 eV overall compared to the undoped Cs<sub>2</sub>ZnCl<sub>4</sub> NCs, and the spectral peaks were shifted to the right, reflecting the change in the chemical environment of the internal structure of the Bi-doped Cs<sub>2</sub>ZnCl<sub>4</sub> NCs and the increase in the electron density.

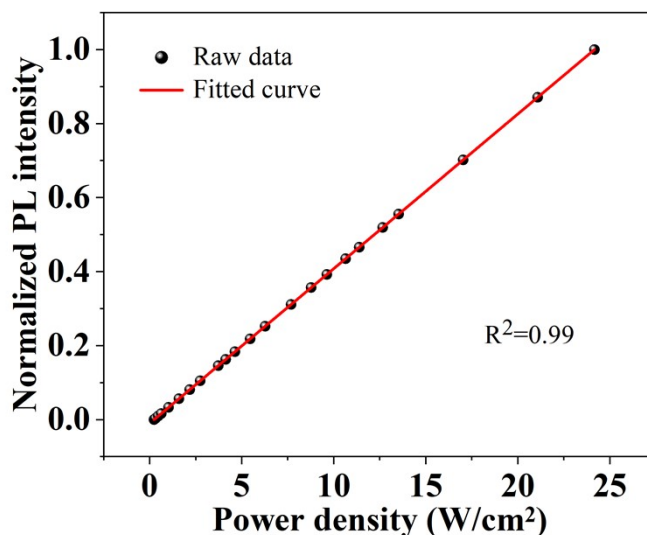


**Fig. S5.** Emission intensity versus excitation power for Cs<sub>2</sub>ZnCl<sub>4</sub>:3%Bi NCs.

The PL intensity of Bi-doped Cs<sub>2</sub>ZnCl<sub>4</sub> NCs exhibit linear relationship with their excitation power, thus excluding the possibility of permanent defects as the origin of photoemission.

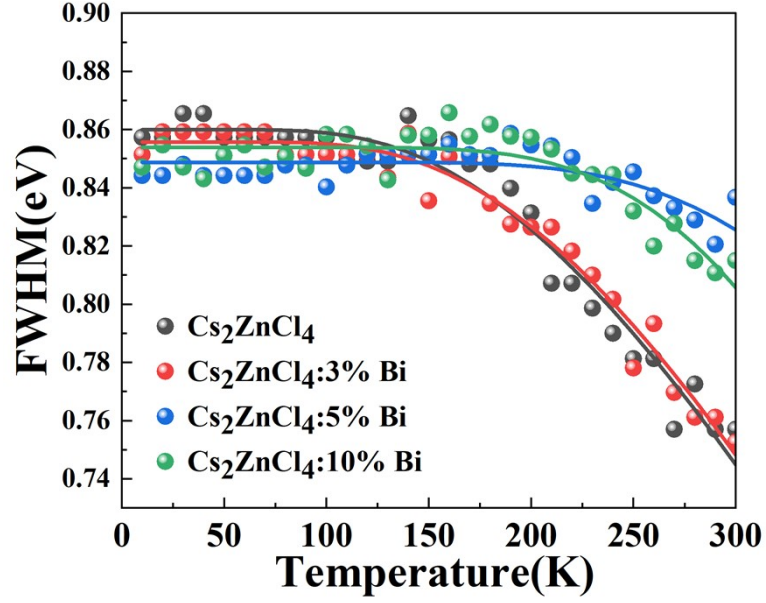


**Fig. S6.** Fitting results of the FWHM of the PL spectra as a function of temperatures for  $\text{Cs}_2\text{ZnCl}_4:\text{Bi}$  NCs with different  $\text{Bi}^{3+}$  concentrations.

**Note:** the temperature dependent FWHM is fitted by the following equation :

$$\Gamma(T) = \Gamma_0 + \Gamma_{op} / \left( e^{\eta\omega_{op}/k_B T} - 1 \right)$$

where  $\Gamma_0$  is the intrinsic line width at absolute temperature 0 K,  $\Gamma_{op}$  is the electron-optical phonon coupling energy,  $\eta\omega_{op}$  is the longitudinal optical phonon energy,  $k_B$  is the Boltzmann constant.

a

b



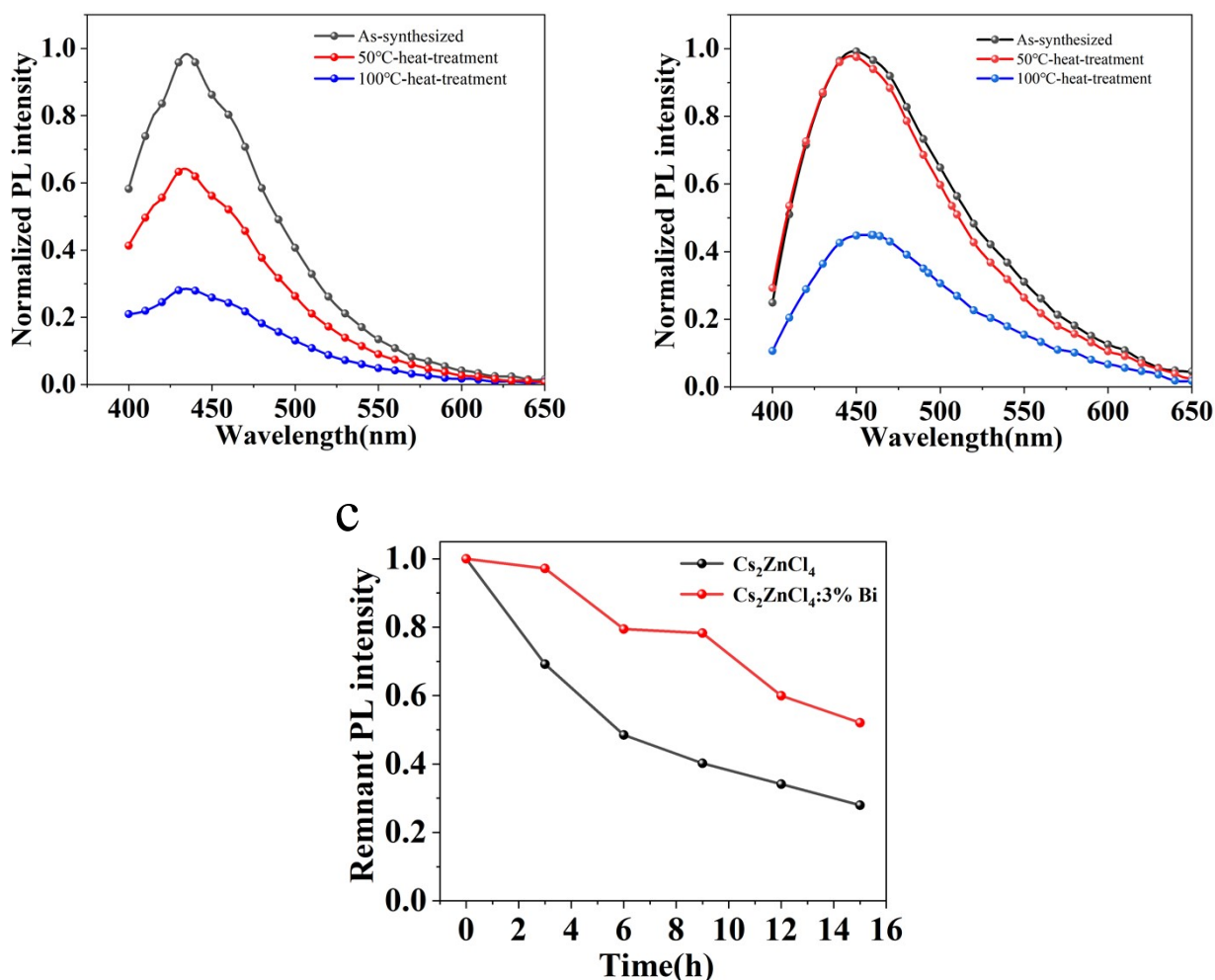


**Fig. S7.** Normalized PL spectra of heat-treated (a)  $\text{Cs}_2\text{ZnCl}_4$  and (b)  $\text{Cs}_2\text{ZnCl}_4:3\%\text{Bi}$  NCs. The duration for both 50 °C and 100 °C was 30 min; and all PL measurements were done at room temperature. (c) Optical stability of  $\text{Cs}_2\text{ZnCl}_4$  and (b)  $\text{Cs}_2\text{ZnCl}_4:3\%\text{Bi}$  NCs. The light source is 365nm UV light.

The PL intensity of  $\text{Cs}_2\text{ZnCl}_4:3\%\text{Bi}$  NCs was only 28% of the initial value under heat treatment at 100 ° C for 30 min, while  $\text{Cs}_2\text{ZnCl}_4:3\%\text{Bi}$  NCs still maintained 45% of the initial PL value (Fig. S7 a,b). In addition,  $\text{Cs}_2\text{ZnCl}_4$  and  $\text{Cs}_2\text{ZnCl}_4:3\%\text{Bi}$  NCs were tested for photostability. Under the continuous irradiation of a UV lamp with a power of 3 W, a fluorescence spectrometer was used to measure the PL intensity in the blue light region of the samples after different irradiation times. The PL intensity of the undoped samples decayed faster than that of the Bi-doped samples. After 15 hours of irradiation, the PL intensity of  $\text{Cs}_2\text{ZnCl}_4$  NCs retained 27% of the initial value, while  $\text{Cs}_2\text{ZnCl}_4:3\%\text{Bi}$  NCs retained 52% of the initial value (Fig. S7 c).

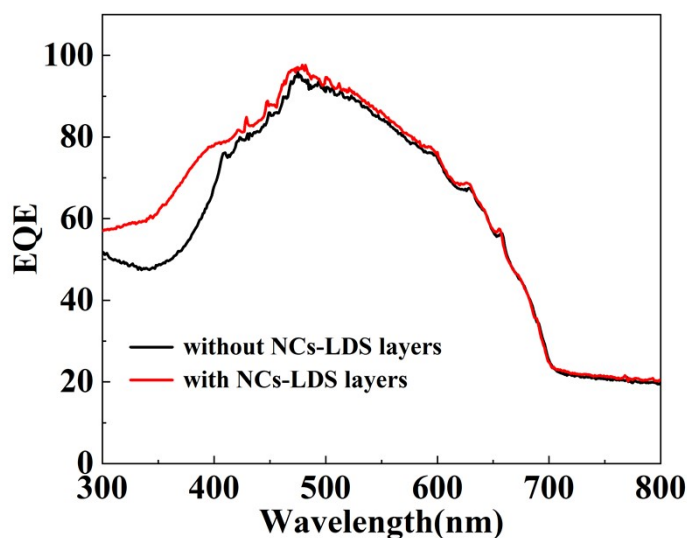


**Fig. S8.** EQE spectra of GaAs solar cells with and without NCs-LDS layer

As shown in Fig. 3, the EQE of GaAs solar cells with NCs-LDS layer increases significantly in the 300-400 nm range, which may be ascribed to the down-conversion effect of Bi-doped  $\text{Cs}_2\text{ZnCl}_4$  nanocrystals. Nanocrystals can absorb photons in the UV range and transform them to visible light. The transformed photons are subsequently delivered to the solar cell, which improves the light response in the short wavelength area and consequently the conversion efficiency.

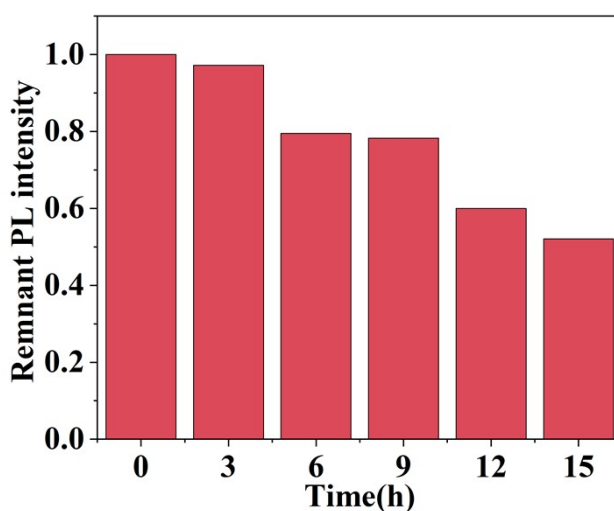


**Fig. S9.** The stability of as-fabricated LED device

Fig S9 shows the stability test of the as-fabricated LED device. After 15 hours of continuous lighting, the blue emission intensity of LED is 52% of the initial value.

To make blue-light LED devices, the produced  $\text{Cs}_2\text{ZnCl}_4\text{:Bi}$  NCs were evenly blended with epoxy glue and covered on a commercial 365 nm GaN LED chip before being dried and cured.

**Table S1.** Composition of Bi-doped Cs<sub>2</sub>ZnCl<sub>4</sub> NCs measured by TEM-EDS instrument. The amount of different elements was expressed relative to that Zn, which was assumed to be 1.

<b>Bi/Zn molar feed ratio</b>	<b>TEM-EDS analysis</b>	
	<b>Composition</b>	<b>Bi/Zn (%)</b>
0:1	Cs <sub>1.5</sub> ZnCl <sub>0.5</sub>	/
0.01:1	Cs <sub>2.9</sub> ZnCl <sub>0.1</sub>	0.24
0.03:1	Cs <sub>1.4</sub> ZnCl <sub>2.0</sub>	0.35
0.05:1	Cs <sub>1.5</sub> ZnCl <sub>1.1</sub>	0.50
0.1:1	Cs <sub>1.8</sub> ZnCl <sub>2.7</sub>	2.33
0.2:1	Cs <sub>3.4</sub> ZnCl <sub>6.5</sub>	3.72